

THIS DOCUMENT CONTAINS
POOR QUALITY PAGES

PRELIMINARY

Accession No. _____

Contract Program or Project Title:

Subject of this Document:

223
TFBP-TR-207 → Effects of Annealing of Irradiation Damage
and Cold Work on Cladding Plastic Deformation

Type of Document:

Author(s), Affiliation and Address:

D. L. Hagrman, EG&G Idaho, Inc.
Box 1625
Idaho Falls, ID 83401

Contract No.:

Date of Document:

October 1977

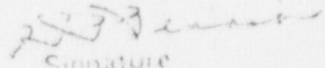
Date Transmitted to NRC:

November 15, 1977

NRC Individual and NRC Office or Division to Whom Inquiries Should be Addressed
S. Fabric
Analysis Development

This document was prepared primarily for preliminary or internal use. It has not received full NRC review and approval. Since there may be substantive changes, this document should not be considered final.

This Document may be made Publicly Available:


Signature

(NRC Program or Project Sponsor or
Authorized Contractor Official)

U.S. Nuclear Regulatory Commission
Washington, D. C. 20555

PRELIMINARY

781107 0189

bcc: J. G. Crocker
J. A. Dearien
C. O. Doucette
D. L. Hagman
J. C. Haire
R. W. Marshall, Jr.
G. L. Schulz
H. B. Woolley, II
L. J. Ybarrondo
J. O. Zane
R. A. DaBell, w/o attach.
Central Files

January 11, 1978

Mr. R. E. Tiller, Director
Reactor Operations and Programs Division
Idaho Operations Office - DOE
Idaho Falls, Idaho 83401

REPORT NUMBER REVISION - Zan-7-78

Ref: J. O. Zane ltr to R. E. Tiller, Zan-327-77, Transmittal of Report -
Effects of Annealing of Irradiation Damage and Cold Work on Cladding
Plastic Deformation, October 21, 1977

Dear Mr. Tiller:

Attached is a reissue of the cover of the report transmitted by the
reference with a corrected report number.

Very truly yours,

Original Signed By

J. O. Zane, Manager
Thermal Fuels Behavior Program

DLH/dk

Attachment:
As stated

cc: R. W. Barber, DOE-RSRC - 2
R. B. Foulds, NRC-RSR
W. V. Johnston, NRC-RSR - 2
R. Rossi/J. E. Humphreys, NRC-OMIPC
P. O. Strom, NRC-ID
L. S. Tong, NRC-RSR
R. W. Kiehn, EG&G Idaho w/o attach.

NRC Research and Technical
Assistance Report

EFFECTS OF ANNEALING OF IRRADIATION DAMAGE AND COLD WORK ON CLADDING PLASTIC DEFORMATION

November 1977

NRC Research and Technical
Assistance Report



EG&G Idaho, Inc.



IDAHO NATIONAL ENGINEERING LABORATORY

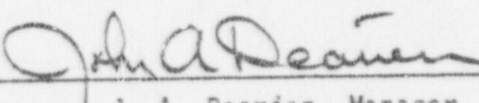
DEPARTMENT OF ENERGY

IDAHO OPERATIONS OFFICE UNDER CONTRACT EY-76-C-07-1570

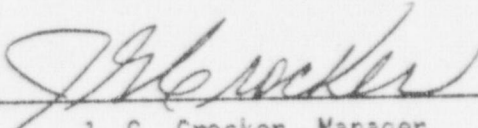
EFFECTS OF ANNEALING OF IRRADIATION DAMAGE AND
COLD WORK ON CLADDING PLASTIC DEFORMATION

Prepared By
Donald L. Hagrman

APPROVALS:



J. A. Dearien, Manager
Fuel Analysis Research and Development Branch



J. G. Crocker, Manager
Thermal Fuels Behavior Division

THERMAL FUELS BEHAVIOR PROGRAM
EG&G Idaho, Inc.

EFFECTS OF ANNEALING OF IRRADIATION DAMAGE AND COLD WORK ON CLADDING PLASTIC DEFORMATION

October 1977

NRC Research and Technical
Assistance Report



EG&G Idaho, Inc.



IDAHO NATIONAL ENGINEERING LABORATORY

ENERGY RESEARCH AND DEVELOPMENT ADMINISTRATION

IDAHO OPERATIONS OFFICE UNDER CONTRACT EY-76-C-07-1570


TFBP-TR-207
October 1977

EFFECTS OF ANNEALING OF IRRADIATION DAMAGE AND
COLD WORK ON CLADDING PLASTIC DEFORMATION

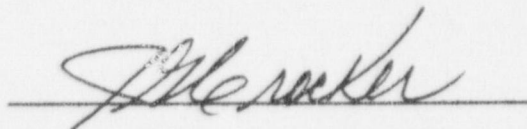
Prepared By

Donald L. Hagrman

APPROVALS:

A handwritten signature in dark ink, appearing to read "J. A. Dearien", is written over a horizontal line.

J. A. Dearien, Manager
Fuel Analysis Research and Development Branch

A handwritten signature in dark ink, appearing to read "J. G. Crocker", is written over a horizontal line.

J. G. Crocker, Manager
Thermal Fuels Behavior Division

THERMAL FUELS BEHAVIOR PROGRAM

EG&G Idaho, Inc.

FOREWORD

This report describes work which is part of the fuel rod behavior modeling task performed at EG&G Idaho, Inc. It is an extension of work previously published in the materials properties (MATPRO) Handbook^[a] and will be incorporated into Section B-8 (cladding stress versus strain) of the MATPRO 09 handbook.

The material property correlations and computer subcodes described in MATPRO are developed for use in Light Water Reactor (LWR) analytical programs such as the Fuel Rod Analysis Program -- Steady-State (FRAP-S3)^[b] code and the Fuel Rod Analysis Program--Transit (FRAP-T3)^[c] code. This work is being performed as part of a broad effort to develop and verify analytical models capable of describing nuclear fuel rod behavior.

The format and numbering scheme used in this report is consistent with its intended use as part of the eighth section of Appendix B of the MATPRO 11 description. The revised section will also include material from a previous report^[d].

- [a] P. E. MacDonald and L. B. Thompson (EDs.) MATPRO Version 09 - A Handbook of Materials Properties For Use in the Analysis of Light Water Reactor Fuel Rod Behavior, TREE-NUREG-1005 (December 1976).
- [b] J. A. Darien, et al., FRAP-S3: A Computer Code for Steady-State Analysis of Oxide Fuel Rods - Vol 1 - Analytical Models and Input Manual, TFBP-TR-164 (January 1977).
- [c] J. A. Dearine, et al., FRAP-T3: A Computer Code for Transient Analysis of Oxide Fuel Rods, TFBP-TR-194 (August 1977).
- [d] Donald L. Hagerman and Gregory A. Reymann, Cladding Stress Versus Strain (CSTRES and CSIGMA), TFBP-TR-193 (April 1977).

CONTENTS

FOREWORD.	
8.5 Effects of Annealing of Irradiation Damage and Cold Work on Cladding Plastic Deformation.	1
8.5.1 Summary.	1
8.5.2 Available Data	4
8.5.3 Model Development.	13
8.5.4 Comparison of Model With Data.	27
8.5.5 Recommendations for Future Modeling and Experiments.	31
8.5.6 Listing of the Subcode CKMN and Examples of Output	32
8.6 References	46
APPENDIX A RELATION BETWEEN ISOTHERMAL AND TRANSIENT ANNEALING EXPRESSIONS.	48

TABLES

B-8.I Room Temperature Ultimate Strengths of Cladding Annealed for One Hour by Howe and Thomas.	6
B-8.II 644 K Test Results for Unirradiated Transient-Annealed Cladding.	8
B-8.III 644 K Test Results with Irradiated Transient-Annealed Cladding.	9
B-8.IV 644 K Test Results with Irradiated Isothermally Annealed Cladding.	10
B-8.V Strength Coefficient and Residual Strength Coefficient After Isothermal Anneals.	18
B-8.VI Strength Coefficient and Residual Strength Coefficient with Modified Cold Work Annealing Model	20

B-8.VII	Strength Coefficient and Residual Strength Coefficient After Transient Anneals	21
B-8.VIII	Strength Coefficient and Residual Strength Coefficient After Transient Anneals	22
B-8.IX	Comparison of Model Predictions with Data Base for Unirradiated Cladding	28
B-8.X	Comparison of Model Predictions with Data Base for Transient Anneals of Irradiated Cladding.	29
B-8.XI	Comparison of Model Predictions with Data Base for Isothermal Anneals of Irradiated Cladding	30
B-8.XII	Listing of the Subcode CKMN	33

8.5 Effects Of Annealing of Irradiation Damage And Cold Work On Cladding Plastic Deformation^[a]

Materials properties (MATPRO) correlations which describe zircaloy cladding plastic deformation have been modified to provide an improved description of the annealing of cold work and irradiation effects. Previous correlations predicted fractional losses of cold work and fluence which were dependent only on the maximum temperature reached by the cladding^[8-8.1]. The present version of the model describes the annealing of cold work and irradiation damage as a function of the time and temperature history of the cladding.

This revised annealing model is based primarily on early data from a program at Battelle Columbus Laboratories titled "Evaluating Strength and Ductility of Irradiated Zircaloy" which is being sponsored by the nuclear regulatory commission^[B-8.2-B-8.9]. The model will be revised or entirely replaced by a model which will be constructed as part of the Battelle Columbus program. Meanwhile, the present model will help assess the effect of time dependent annealing kinetics on code predictions of such properties as cladding strength and cladding circumferential elongation at failure.

8.5.1 Summary. Data from the BCL program imply not only complex annealing kinetics but also an effect of fast neutron fluence on the strength coefficient which had not been modeled in MATPRO. The preliminary correlation for this effect which has been incorporated into the MATPRO subcodes for plastic deformation is

$$K_{\phi} = 4.68 \times 10^{-18} \phi \quad (B-8.1)$$

Where K_{ϕ} = change in strength coefficient due to irradiation
(newtons/meter²)

ϕ = fast neutron fluence (meters⁻²)

[a] This report is intended to supplement and later be incorporated into a revision of Section 8 Appendix B of the MATPRO handbook.

Changes in the strength coefficient and strain hardening exponent caused by cold work and irradiation anneal according to separate rate equations. The progress of this annealing is described by keeping track of effective cold work and effective fast neutron fluence for use in previously developed correlations for the strength coefficient and strain hardening exponent [B-8.1].

The ratio effective cold work for the strength coefficient at the end of a time step divided by effective cold work at the beginning of an isothermal time step is

$$FK = \exp \left[-1.504 \left(1 + 2.2 \times 10^{-25} \phi_{K0} \right) t \exp \left(\frac{-2.33 \times 10^{18}}{T^6} \right) \right] \quad (B-8.2)$$

Where FK = effective cold work for strength coefficient at the end of a time step divided by effective cold work at the beginning of a time step

ϕ_{K0} = effective fast neutron fluence for strength coefficient at the start of the time step (neutrons/meter²)

t = time step size (sec)

T = cladding temperature (K)

The effective fast neutron fluence for calculating the strength coefficient after an isothermal time step is computed with the expression

$$\frac{1}{\phi_K} = 2.11 \times 10^{-6} t \exp \left(\frac{-5.35 \times 10^{23}}{T^8} \right) + \frac{1}{\phi_{K0}} \quad (B-8.3)$$

Where ϕ_K = effective fast neutron fluence for strength coefficient at the end of a time step (neutrons/meter²)

ϕ_{K0} = effective fast neutron fluence for strength coefficient at the start of the time step (neutrons/meter²)

t = time step size (sec)

T = cladding temperature (K)

The ratio effective cold work for the strain hardening exponent at the end of a time step divided by effective cold work for strain hardening exponent at the beginning of an isothermal time step is

$$FN = \exp \left[-15.04 \left(1 + 2.2 \times 10^{-25} \phi_{NO} \right) t \exp \left(\frac{-2.33 \times 10^{18}}{T^6} \right) \right] \quad (B-8.4)$$

Where FN = effective cold work for strain hardening exponent at the end of a time step divided by effective cold work for strain hardening exponent at the beginning of a time step

ϕ_{NO} = effective fast neutron fluence for the strain hardening exponent at the start of the time step (neutrons/meter²)

t = time step size (sec)

T = cladding temperature (K)

The effective fast neutron fluence for calculating the strain hardening exponent after an isothermal time step is computed with the expression

$$\frac{1}{\phi_N} = 1.054 \times 10^{-4} t \exp \left(\frac{-5.35 \times 10^{23}}{T^8} \right) + \frac{1}{\phi_{NO}} \quad (B-8.5)$$

Where ϕ_N = effective fast neutron fluence for strain hardening exponent at the end of a time step (neutrons/meter²)

ϕ_{NO} = effective fast neutron fluence for strain hardening exponent at the start of the time step (neutrons/meter²)

t = time step size (sec)

T = cladding temperature (K)

If the time step is not isothermal, equations B-8.2 to B-8.5 must be modified to include the effect of varying temperature. The appropriate modification is to replace the exponential function of temperature in each of the equations by the factor shown below

$$\exp\left(\frac{-Q}{T^m}\right) \rightarrow \left[\exp\left(\frac{-Q}{T_0^m}\right) \left[\exp\left(\frac{Q}{T_0^{m+1}} \frac{dT}{dt} t\right) - 1 \right] \right] \quad (\text{B-8.6})$$

Where Q, m = the constants which appear in the isothermal expression

T_0 = temperature at the start of the time step (K)

t = time step size (sec)

$\frac{dT}{dt}$ = average rate of change of temperature expected during the time step. (K/sec)

Expression B-8.6 is the exact expression for a constant rate of temperature change and is only an approximation for non-linear temperature changes.

The available data are reviewed in Section 8.5.2 and correlations are developed in Section 8.5.3. Section 8.5.4 is a comparison of model predictions with the data base. Several recommendations for future modeling work and future experiments are presented in Section 8.5.5. Sections 8.5.6 and 8.5.7 provide code listings and references.

8.5.2 Available Data. Howe and Thomas have reported post-irradiation annealing studies on annealed, 13.1 percent cold-worked and tempered 25.5 percent cold-worked Zircaloy-2 irradiated at 493 K (220°C) and 553 K (280°C) with integrated fast neutron fluxes of $3.6 \times 10^{23}/\text{m}^2$ and

$2.7 \times 10^{24}/m^2$ [B-8.10]. Specimens were given one hour anneals in vacuum at various temperatures. The nominal room temperature ultimate stresses measured with these samples are reproduced in Table B-8.I.

The data from irradiated annealed Zircaloy-2 shows that irradiation induced hardening in this material is completely annealed out by one hour anneals at temperatures above 775 K (500°C) and that most of the recovery occurs in the temperature range 575-675 K (300-400°C). From their recovery data with 25.5% cold worked Zircaloy-2 Howe and Thomas concluded that:

- (1) the recovery occurring in the temperature range 550 K (280°C) to 725 K (450°C) is the annealing out of irradiation damage rather than cold-work;
- (2) the irradiation damage in cold worked material is completely annealed out by one hour anneals at approximately 725 K (450°C) and
- (3) the recovery from 725 K (450°C) to 973 (700°C) for irradiated material is fairly similar to that for unirradiated material. However, there is an indication that the irradiated material recovers slightly faster.

Since the one hour anneals of Howe and Thomas represent times which are long compared to LOCA (loss of coolant accident) blowdown and refill times, the data were used only for general guidance and verification of the models developed from shorter annealing times reported by Bauer et al. In particular, the data support the ideas that (1) irradiation damage anneals before cold work and (2) irradiation damage affects the rate of annealing of cold work but the effect may be treated as a perturbation of the cold work annealing.

Bauer et al have reported yield strengths, ultimate strength, uniform elongations (engineering strain at maximum load), and total elongations from annealing studies of both cold worked and irradiated

TABLE 8.1

ROOM TEMPERATURE ULTIMATE STRENGTHS OF CLADDING
ANNEALED FOR ONE HOUR BY HOWE AND THOMAS

Cold Work (%)	Fluegge (n/m ²)	Annealing Temperature (K)	Ultimate Strength (MPa)
0	3.6×10^{23}	555	634
0	3.6×10^{23}	625	588
0	3.6×10^{23}	675	513
0	3.6×10^{23}	725	513
0	3.6×10^{23}	775	500
0	3.6×10^{23}	875	500
0	3.6×10^{23}	975	499
25.5	0	555	619
25.5	0	675	614
25.5	0	775	603
25.5	0	875	530
25.5	0	975	512
25.5	2.7×10^{24}	555	728
25.5	2.7×10^{24}	625	712
25.5	2.7×10^{24}	675	675
25.5	2.7×10^{24}	725	626
25.5	2.7×10^{24}	775	579
25.5	2.7×10^{24}	875	504
25.5	2.7×10^{24}	975	486

cold worked zircaloy cladding material^[B-8.6-B-8.7]. The unirradiated cold worked cladding was from a standard lot of tubing which has been characterized by R. H. Chapman^[B-8.11]. The irradiated cladding was obtained from spent fuel rods irradiated in the Carolina Power and Light H. B. Robinson Plant to a fast neutron fluence of approximately 4.4×10^{25} /meter².

Ultimate strengths and uniform elongations obtained at 644 K (700°F) and a strain rate of 0.025/min with the unirradiated cladding are reproduced in Table B-8.II. With a heating rate of 5.6 K/sec most of the recovery of both strength and uniform elongation occurs between temperatures of 894 and 978 K. However, the recovery has barely started at 978 K when the heating rate is 27.8 K/sec. Since the annealing times at temperature are short, the maximum temperature required to anneal these samples is considerably higher than the temperatures reported by Howe and Thomas.

Tables B-8.III and B-8.IV are a summary of Bauer et al's measurements of ultimate strengths and uniform elongations of annealed irradiated tubing. The measurements were performed at 644 K (700°F) and a strain rate of 0.025/min. The results in Table B-8.III were obtained with transient anneals similar to the anneals used with the unirradiated tubing. Table B-8.IV summarizes results from isothermal anneals which are similar to the anneals carried out by Howe and Thomas.

The annealing behavior of the irradiated cladding is different than the behavior of the unirradiated material. Ultimate strengths obtained with irradiated material which had little or no annealing are substantially higher than the ultimate strengths of the unirradiated material. However, transient anneals which begin to affect the strength of cold worked material (5.6 K/sec to 866 and 894 K or 27.8 K/sec to 978 K) leave the irradiated material with strengths which are below the strengths of the unirradiated material after corresponding anneals. It is possible that these differences are due to the fact that the tubing does not come from

TABLE 8. II

644 K TEST RESULTS FOR UNIRRADIATED TRANSIENT-ANNEALED CLADDING

Specimen Number	Heating Rate (K/sec)	Maximum Temperature (K)	Ultimate Strength (MPa)	Uniform Elongation (percent)
as received	---	644	434.5	4.1
0781-8	5.6	811	434	4.1
-7	5.6	866	432	4.1
-6	5.6	894	409	4.8
-5	5.6	978	252	24.3
-4	27.8	811	434	3.6
-3	27.8	866	438	3.3
-2	27.8	894	432	3.6
-1	27.8	978	422	4.6

TABLE 8.III

644 K TEST RESULTS WITH IRRADIATED TRANSIENT-ANNEALED CLADDING

Specimen Number	Heating Rate (K/sec)	Maximum Temperature (K)	Ultimate Strength (MPa)	Uniform Elongation (percent)
P8-20	---	644	622.8	4.1
P8-34	---	644	650.3	4.0
P8-46	---	644	660.9	2.8
H10-20	---	644	694.0	3.8
P4-50-55	0.6	700	674	2.1
P4-55-60	0.6	755	633	2.7
P4-89-1/2-94-1/2	0.6	811	574.5	2.3
P4-94-1/2-99-1/2	0.6	894	286.1	9.57
Pr-99-1/2-104-1/2	0.6	978	268.9	9.21
P4-111-116	5.6	700	653	2.0
P4-45-50	5.6	755	676	2.4
P4-35-3/4-46-3/4	5.6	811	595.2	2.35
Pr-70-3/4-75-3/4	5.6	866	349.3	2.94
Pr-75-3/4-80-3/4	5.6	894	313.7	4.77
Pr-80-1/2-89-1/2	5.6	978	287.3	10.56
O14-106-1/2-111-1/2	13.9	755	717	2.4
A8-120-3/4-125-3/4	13.9	811	652.7	2.27
P4-16-1/2-21-1/2	13.9	866	577.9	2.50
P4-21-1/2-26-1/2	13.9	894	456.2	2.16
P4-26-1/2-31-1/2	13.9	978	304.5	5.74
P4-65-70	27.8	755	671	2.1
A1-29-1/2-34-1/2	27.8	811	721.6	2.70
A8-105-3/4-110-3/4	27.8	866	671.0	2.70
A8-110-3/4-115-3/4	27.8	894	597.5	2.06
A8-115-3/4-120-3/4	27.8	978	348.2	3.49
P4-116-21	27.8	1033	329	4.7
O14-111-1/2-116-1/2	27.8	1144	338	8.6
O14-37-42	27.8	1255	340	10.5

TABLE 8.IV

644 K TEST RESULTS WITH IRRADIATED ISOTHERMALLY ANNEALED CLADDING

Specimen Number	Temperature (K)	Time at Temperature (min)	Ultimate Strength (MPa)	Uniform Elongation (percent)
P8-20	644	---	622.8	4.1
P8-34	644	---	650.3	4.0
P8-46	644	---	660.9	2.8
H10-20	644	---	694.0	3.8
H10-5	700	60	615.9	3.35
H10-41	755	10	590.6	2.85
H10-17	755	60	556.2	3.06
P4-60-65	811	1	560	2.9
A1-24-1/2-29-1/2	811	10	363.1	3.2
H10-18	811	30	371.1	5.10
A1-105-3/4-110-3/4	866	1	332.1	4.52
A1-99-104	866	5	311.4	8.03
H10-3	866	30	321.7	10.1
A1-110-3/4-115-3/4	894	1	308.9	7.90
H10-4	894	30	319.4	13.93
A1-116-1/2-121-1/2	978	1	305.6	7.67
H10-16	978	30	311.4	11.80

the same lot but a similar trend has been shown by the studies of Howe and Thomas on material from one lot. This author has thus concluded that irradiation for long times at reactor operating temperatures causes a significant increase in the strength of zircaloy cladding and enhances the annealing of the strength increase due to cold work.

Comparison of uniform elongation measurements with the unirradiated and irradiated cladding (Tables 8.5.II and 8.5.III) shows that the effect of irradiation on this parameter may be different than its effect on ultimate strength. The uniform elongation of the unannealed irradiated material is less than the uniform elongation of the unannealed unirradiated material but there is no obvious increase in the rate of recovery from cold work effects because of the irradiation. Therefore, models which describe annealing by keeping track of effective cold work and effective fluence should be set up to use different values of these parameters for predicting strength and elongation.

The isothermal annealing effects reproduced in Table 8.IV are similar to those of Table 8.III in that recovery of ultimate strength preceeds recovery of uniform elongation. However, several additional features of the annealing of cold worked and irradiated zircaloy cladding become apparent from the isothermal data.

- (1) The four tests at 644 K show that approximately 10% sample-to-sample scatter should be expected in the measured values of strength. In particular, rod H10^[a] shows consistently high values of strength. Variation of the order of a percent seems to be present in the uniform elongation data. Models for annealing will therefore have to emphasize general trends and avoid exact fits to individual measurements.

[a] The first part of the specimen numbers in Tables B-8.II-B-8.IV identify the rod from which the specimen was taken.

- (2) Irradiation effects on the strength of zircaloy cladding do not seem to saturate at the low values of fluence used by Howe and Thomas. The two sixty minute anneals show strengths at 644 K which are similar to the room temperature strengths measured after similar anneals by Howe and Thomas. If the tensile test data had been taken at similar temperatures, the cladding measured by Bauer would show considerably greater strength.
- (3) Time at temperature during annealing is less important for the irradiated material than for the unirradiated material. The model which will be developed in Section 8.5.3 for annealing of the effect of cold work on strength will predict that the log of the departure of strength parameters from their annealed values for two isothermal anneals which differ only in the time at temperature should be proportional to the reciprocal ratio of the annealing times. The major component of the increase of the strengths in Table 8.5.IV is much less dependent on time at temperature than this relation would imply^[a].

The net impression left by the data of Tables 8.I to 8.IV is that at least two different processes are important in the annealing of cold worked and irradiated cladding and that the annealing of the irradiation caused component follows a rate equation which is different than the rate equation for the cold work component. Data which could be used to model these separate processes (e.g. annealing studies with one lot of material irradiated to several different fluences) are not available. Therefore the model developed in the next section will be a strictly empirical attempt to reproduce the data we do have with a reasonably concise set of correlations.

[a] For example, the ten and sixty minute anneals at 775 K have ultimate strengths which are 279.2 and 244.8 MPa above the fully annealed ultimate strength of sample H10-16. An equation with the form of Equation B-8.2 would imply that the ratio of the logs of the two strengths should be 1/6 or 0.17. The ratio is 0.98.

8.5.3 Model Development. The approach used to develop the annealing models presented here was to develop a model for the annealing of cold worked cladding and to modify this model to fit data from cold worked and irradiated material. The model for recovery kinetics in cold worked cladding is based on the suggestion by Byrne^[B-8.12] that recovery^[a] data frequently conform to the assumption that the rate of recovery of a property from its cold worked value is proportional to the instantaneous value of the property. If the property in question is the strength coefficient^[b] the rate equation for recovery is

$$\frac{dK}{dt} = - f_T [K - K_A] \quad (B-8.7)$$

Where K = strength coefficient of cold worked cladding (MPa).

K_A = strength coefficient of annealed cladding (MPa)

t = time

f_T = a temperature dependent factor

Since isothermal annealing data with unirradiated cold worked tubing are not available, the affect of temperature on the factor f_T in equation B-8.7 had to be determined from the limited transient annealing data of Table 8.II. The method used to do this is outlined below and in the Appendix.

[a] A separate model for recrystallization kinetics was developed but not used because only limited recrystallization data are available. Moreover, recrystallization effects do not appear to be important in predicting plastic deformation parameters for typical LOCA transients.

[b] Since the change in the strength coefficient is modeled as a linear function of cold work^[B-8.1], one could use cold work instead of the strength coefficient in this equation.

- (1) The change of the factor f_T in Equation B-8.7 was assumed to be represented by an expression of the form

$$f_T = B \exp \left(\frac{Q}{T^m} \right) \quad (\text{B-8.8})$$

Where B, Q , and m = positive constants

T = temperature (K)

- (2) Equation B-8.7 was integrated over a very short (approximately isothermal) time interval to produce a differential expression for the change in strength coefficient.
- (3) The long interval beginning at a temperature T_i and ending at a temperature T_f was divided into several approximately isothermal intervals with temperatures obtained by linear interpolation between T_i and T_f .
- (4) An expression for the net change in the strength coefficient due to the several short intervals was written.
- (5) The limit of the expression for the net change in the strength coefficient as the number of short intervals approaches infinity was determined. The limit is

$$\frac{K_f - K_A}{K_i K_A} = \exp \left(-B \left[\exp \left(\frac{-Q}{T_f^m} \right) \right] \left[\frac{1 - \exp \left(\frac{-Q [T_f - T_i] m}{T_f^{m+1}} \right)}{\frac{Q [T_f - T_i] m}{T_f^{m+1}}} \right] [t_f - t_i] \right) \quad (\text{B-8.9})$$

where the subscript i refers to the initial value and subscript f refers to the final value of the quantities which have been defined in conjunction with equations B-8.7 and B-8.8.

- (6) Ultimate strengths and uniform elongations from Table 8.II were used to determine the strength coefficient^[a] after the various anneals described in this table.

[a] The procedure used to determine a strength coefficient from ultimate strength and uniform elongation data is discussed in Reference B-8.1.

- (7) The values of K_f after the anneals to 866 and 894 K at 5.6 K/sec were used with the value of K_i from the as-received material and equation B-8.9 to determine B and Q with assumed trail values of K_A between 364 and 442 MPa and assumed trial integral values of m between 1 and 9.
- (8) Finally, the values of Q, B, K_i , K_A and m for each trial were used in equation B-8.9 to predict K_f for the six anneals which were not considered in step 7. The predictions were compared with the data. The trail values of K_A and m which most successfully predicted both the post-anneal data and the as received strength coefficient (using the stress relief annealing schedule provided in Reference B-8.11) were $K_A = 406$ MPa and $m = 6$. The value $m = 6$ and the values of Q and B which produced the successful predictions ($Q = 2.33 \times 10^{18}$ and $B = 1.504$) were therefore adopted for the model.

A separate model for the annealing of the strain hardening exponent was developed but the model was not used because the strain hardening exponents obtained from the data of Table 8.II were fit equally well by simply assuming that a slight modification ($B = 15.04$) of the model just developed for the annealing of the cold work contribution to the strength coefficient also applies to the cold work term in the expression^[a] which is used in MATPRO to model the effect of cold work on the strain hardening exponent.

The rest of this section describes the development of models for the annealing of cold worked and irradiated cladding. It was concluded in Section 8.5.2 that the principal features of the annealing data with irradiated cladding are

- (1) the large previously unmodeled increase in strength with irradiation,
- (2) the increased rate of recovery from cold work effects when material has been irradiated and

[a] Equations 10 and 11 of Reference B-8.1.

- (3) the apparent difference between the annealing kinetics of cold work damage and the annealing kinetics of the irradiation caused increase in strength.

The modeling of these features will be addressed in the order of the above list.

The first step in producing a model for these effects was to estimate the magnitude of the increase in strength coefficient with irradiation. The cold work contribution to the change in the strength of the irradiated cladding was estimated from nominal preirradiation values of the ultimate strength and uniform elongation at room temperature and at 658 K (725°F)^[B-8.8]. The two estimates of cold work, 0.65 and 0.72, were averaged and the resultant estimate of the cold work contribution at the test temperature, 644°K was calculated using the MATPRO correlation for the effect of cold work on the strength coefficient^[B-8.1].

Finally, the cold work contribution to the strength coefficient and the annealed state strength coefficient for each of the tubes used in the four tests of as received cladding^[a] were subtracted from the strength coefficients obtained from the data in Table 8.IV. The resultant values for the irradiation contribution to the strength coefficient were 191.7, 222.5, 204.4 and 205.9 MPa. The average of these numbers was divided by the average fast neutron fluence received by the H. B. Robinson rods, $4.4 \times 10^{25}/\text{meter}^2$ ^[B-8.4], to produce a crude correlation for the effect of irradiation on the strength coefficient:

$$K_{\phi} = 4.68 \times 10^{-18} \phi \quad (\text{B-8.10})$$

Where K_{ϕ} = change in strength coefficient due to irradiation
(newtons/meter²)

ϕ = fast neutron fluence (meters⁻²)

[a] The four samples were P8-20, P8-34, P8-46 and H10-20. A value of 406 MPa was used for the annealed strength of the samples from rod P8 and 452.5 MPa was used for the sample from rod H10. The value for rod H10 is based on the strength coefficient measured with sample H10-16 and is anomalously high.

The second step in producing a model for the annealing of irradiated cladding was to modify the model for cold work annealing to include the irradiation-caused enhancement of the recovery of the strength coefficient from cold work effects. The modification of the cold work annealing model is based on the information in Table 8.V^[a]. The first two columns identify the annealing tests and column three is the strength coefficients calculated from the ultimate strengths and uniform elongations of Bauer's isothermal annealing tests (Table 8.IV). The column titled residual strength coefficient is the strength coefficient minus the sum of the strength coefficient for annealed cladding and the contribution of cold work calculated with the unmodified model for cold work annealing. The column titled CW/CW_0 is the initial cold work divided into the post-anneal cold work predicted by the unmodified cold work annealing model. Comparison of the residual strengths and the column titled CW/CW_0 shows that the residual strength coefficient is negative whenever the cold work is predicted to be partly annealed (CW/CW_0 in the range 0.4 to 0.8). The most reasonable interpretation of this feature is to assume that the irradiation enhances the rate of annealing of the cold work. The change required to model this effect is to replace the constant B in equations B-8.8 and B-8.9 by a function which increases with increasing fluence. The expression adopted for the strength coefficient annealing model is

$$B = 1.504 [1 + 2.2 \times 10^{-25} \Phi] \quad (B-8.11)$$

Where B = the rate constant in Equations B-8.8 and B-8.9

Φ = fast neutron fluence (neutrons/meter²)

The procedure just described for determining the effect of irradiation on the annealing of the cold work contribution to the strength coefficient was also carried out for the strain hardening exponent. The procedure

[a] A similar table was constructed from Bauer's transient annealing data. The transient data gave no new information.

TABLE 8.V

STRENGTH COEFFICIENT AND RESIDUAL STRENGTH COEFFICIENT
AFTER ISOTHERMAL ANNEALS

Temperature (K)	Time at Temperature (min)	Strength Coefficient (MPa)	Residual Strength Coefficient (MPa)	CW/CW ₀
644	as received	750.7	191.7	1
644	as received	781.5	222.5	1
644	as received	763.4	204.4	1
644	as received	828.9	205.9	1
700	60	724.8	101.8	1
755	10	683.5	61.0	0.997
755	60	648.2	28.3	0.982
811	1	649.7	94.5	0.975
811	10	425.2	-100.1	0.780
811	30	460.8	- 72.6	0.475
866	1	387.9	-125.1	0.700
866	5	417.2	- 14.3	0.167
866	30	451.6	- 0.9	0.000
894	1	411.3	- 54.7	0.392
894	30	483.2	30.7	0.000
978	1	406.0	0	0.002
978	30	452.5	0	0.000

suggested that equations B-8.8 and B-8.9 can be used to model the annealing behavior of the strain hardening exponent if the constant B is replaced by the expression

$$B = 15.04 [1 + 2.2 \times 10^{-25} \phi] \quad (B-8.12)$$

Where B = the rate constant in Equations B-8.8 and B-8.9

ϕ = fast neutron fluence (neutrons/meter²)

Table 8.VI reproduces the information of Table 8.V using the revised rate constant of equation B-8.10. The residual strength coefficients are close to zero for temperatures above 866 K and for the two long isothermal anneals at 811 K.

The third step in producing a model for the annealing of irradiated cladding is the derivation of expressions to describe the annealing of the residual strength coefficient and the annealing of the effect of fluence on the strain hardening exponent. The expressions for the annealing of the residual strength coefficient are based on the values of this parameter presented in Table 8.VI and on residual strengths obtained with the transient test data of Table 8.III.

Tables 8.VII and 8.VIII are a summary of the strength coefficients and residual strength coefficients obtained with the transient test data. Table 8.VII groups the tests with equal maximum temperature together and Table 8.VIII groups tests with equal heating rates together. Several trends which were used to develop the model for the annealing of the residual strength coefficient are apparent from an inspection of Tables 8.VII and 8.VIII.

Inspection of the data in Table VII shows that the residual strength coefficient does not anneal significantly in any of the tests with a maximum temperature of 755 K. All of the tests with maximum temperature

TABLE 8.VI

STRENGTH COEFFICIENT AND RESIDUAL STRENGTH COEFFICIENT
WITH MODIFIED COLD WORK ANNEALING MODEL

Temperature (K)	Time at Temperature (min)	Strength Coefficient (MPa)	Residual Strength Coefficient (MPa)	CW/CW ₀
644	as received	750.7	191.7	1
644	as received	781.5	222.5	1
644	as received	763.4	204.4	1
644	as received	828.9	205.9	1
700	60	724.8	101.8	1
755	10	683.5	65.8	0.969
755	60	648.2	54.7	0.827
811	1	649.7	239.9	0.025
811	10	425.2	19.2	0.000
811	30	460.8	8.3	0.000
866	1	387.9	- 18.1	0.000
866	5	417.2	+ 11.2	0.000
866	30	451.6	- 0.9	0.000
894	1	411.3	+ 5.3	0.000
894	30	483.2	+ 30.7	0.000
978	1	406.0	0	0.000
978	30	452.5	0	0.000

TABLE 8.VII
STRENGTH COEFFICIENT AND RESIDUAL STRENGTH COEFFICIENT
AFTER TRANSIENT ANNEALS

Heating Rate (K/sec)	Maximum Temperature (K)	Strength Coefficient (MPa)	Residual Strength Coefficient (MPa)	CW/CW ₀
as received	644	750.7	191.7	1
as received	644	781.5	222.5	1
as received	644	763.4	204.4	1
as received	644	828.9	205.9	1
0.6	700	758.5	199.5	1
5.6	700	732.4	173.4	1
0.6	755	728.5	169.7	0.999
5.6	755	769.4	210.4	1.0
13.9	755	816.5	257.5	1.0
27.8	755	755.4	196.4	1.0
0.6	811	651.8	111.0	0.881
5.6	811	676.5	119.5	0.987
13.9	811	739.7	181.5	0.995
27.8	811	830.7	272.1	0.997
5.6	866	405.5	-115.0	0.749
13.9	866	660.5	118.2	0.891
27.8	866	772.4	220.0	0.944
0.6	894	397.0	- 9.0	0.000
5.6	894	385.8	- 79.7	0.389
13.9	894	514.9	4.0	0.685
27.8	894	681.8	149.2	0.828
0.6	978	370.1	- 35.9	0.000
5.6	978	407.1	+ 1.1	0.000
13.9	978	384.9	- 22.4	0.009
27.8	978	411.6	- 8.7	0.932
27.8	1033	403.6	- 2.4	0.001
27.8	1144	458.7	+ 52.7	0.000
27.8	1255	481.1	+ 75.1	0.000

TABLE 8.VIII

STRENGTH COEFFICIENT AND RESIDUAL STRENGTH COEFFICIENT
AFTER TRANSIENT ANNEALS

Heating Rate (K/sec)	Maximum Temperature (K)	Residual Strength Coefficient (MPa)
as received	644	191.7
as received	644	222.5
as received	644	204.4
as received	644	205.4
0.6	700	199.5
0.6	755	169.7
0.6	811	111.0
0.6	894	- 9.0
0.6	978	- 35.9
5.6	700	173.4
5.6	755	210.4
5.6	811	119.5
5.6	866	-115.0
5.6	894	- 79.7
5.6	978	
13.9	755	257.5
13.9	811	181.5
13.9	866	118.2
13.9	894	4.0
13.9	978	- 22.4
27.8	755	196.4
27.8	811	272.1
27.8	866	222.0
27.8	894	149.2
27.8	978	- 8.7
27.8	1033	- 2.4
27.8	1144	+ 52.7
27.8	1255	+ 75.1

of 978 K show essentially complete annealing. The tests with maximum temperatures of 811 K show varying amounts of annealing but the effect of different heating rates (or, said another way, different times at temperature) on the residual strength coefficient is much less than one would expect from an expression like equation B-8.9. If an equation of the form of Equation B-8.9 were used to model the annealing of the residual strength coefficient, the ratio of the logs of the measured residual strength coefficients after two anneals to the same maximum temperature would be predicted to be proportional to the heating rates. The four residual strengths measured after anneals with a maximum temperature of 311 K (where annealing changes are greater than the scatter of the data) show significantly less dependence on heating rate. This observation is supported by the isothermal annealing data of Table 8.VI which also show relatively little dependence on the time at a given temperature.

When the transient data are grouped with equal heating rates together (Table 8.VIII) a very strong dependence of residual strength on maximum temperature is apparent. For all of the heating rates, the annealing of the residual strength occurs over a range of maximum temperatures which is only about 75 K wide. Moreover, the center of this 75 K band is increased by only about 100 K when the heating rate is increased by a factor of 50.

The approach used to model the annealing of the residual strength coefficient was to assume that this component is not subject to the rate equation used for the annealing of cold work effects. The assumption is logical not only because of the information in Tables 8.VI and 8.VIII but also because the probable cause of the residual strength coefficient is radiation damage--vacancies, interstitials, and dislocation loops rather than cold work effects.

In order to describe the annealing of the residual strength coefficient, an empirical rate equation which is a generalized form of equations B-8.7 and B-8.8 was written^[a]

$$\frac{dy}{dt} = B \exp \left(\frac{-Q}{T^m} \right) y^p \quad (B-8.12)$$

Where y = irradiation contribution to the strength coefficient (MPa)

T = temperature (K)

t = time (seconds)

B, Q, m, p = positive constants to be evaluated by comparison to the residual strength coefficient data of Tables 8.VI to 8.VIII

The procedure used with the rate equation for the annealing of cold work effects (Steps (2) to (5) after Equation B-8.8) was repeated with equation B-8.12 to produce a differential expression for the change in y during a time interval with a linear change in temperature. The differential expression is

$$\frac{1}{y_f^{p-1}} = \left[p-1 \right] B \left[\exp \left(\frac{-Q}{T_f^m} \right) \right] \left[\frac{1 - \exp \left(\frac{-Q[T_f - T_i]m}{T_f^{m+1}} \right)}{\frac{Q[T_f - T_i]m}{T_f^{m+1}}} \right] [t_f - t_i] + \frac{1}{y_i^{p-1}} \quad (B-8.13)$$

Where symbols with subscripts i refer to initial values and symbols with subscripts f refer to final values of the symbols in equation B-8.12.

[a] Since the change in the strength coefficient due to irradiation is modeled as a linear function of fast neutron fluence (Equation B-8.1), one could use the fast neutron fluence in place of the variable y in this equation. The net effort would be a change of the constant B .

The author was unable to find a completely analytical method to obtain a best fit of equation B-8.13 to the data. However several observations aided in finding values of B, Q, m and p which provide a fit which is within the scatter of the data.

(1) The factor

$$\frac{1 - \exp\left(\frac{-Q[T_f - T_i]m}{T_f^{m+1}}\right)}{\frac{Q[T_f - T_i]m}{T_f^{m+1}}}$$

can be viewed as a correction for the fact that the temperature did not remain at T_f throughout the anneal. It is not relevant to the fundamental annealing properties of the cladding.

(2) Increasing m increases the sensitivity of the change in y to the temperature because the factor $\exp\left(\frac{-Q}{T_f^m}\right)$ is

more sensitive to temperature when m is larger.

(3) Increasing P decreases the sensitivity of the change in y to the time span $t_f - t_i$. This is most easily seen by noting that for large y_i , y_f is proportional to

$$[t_f - t_i]^{-\frac{1}{p-1}}$$

For large values of p, the $\frac{1}{p-1}$ th root of $t_f - t_i$ is relatively insensitive to $t_f - t_i$.

The residual strength data of Tables 8.VI and 8.VIII were fit by trying integral values of m and p , and using pairs of residual strengths from Table 8.VIII in conjunction with the average value of the as-received residual strength (206 MPa) and equation B-8.13 to solve for trial values of Q and B . Predictions of equation B-8.13 with each trial set of m , p , Q and B were then compared to all the residual strengths of Tables 8.VI and 8.VII. The best fit to the residual strength data was obtained with $m = 8$, $p = 2$, $Q = 5.35 \times 10^{23}$ and $B = 2.11 \times 10^{-6}$ [a].

Two trivial steps were required to convert equation B-8.13 to the form actually used in MATPRO subcodes.

- (1) The equation was transformed to an equivalent expression in terms of the initial temperature and heating rate. This transformation allows all the required input information to be parameters at the beginning of a time-step. The transformation is carried out by using an alternate linear interpolation for temperature as noted in the Appendix.
- (2) The equation was modified to express the change in residual strength in terms of an effective fluence for use in equation B-8.1. The modification was carried out by replacing y in equations B-8.12 and B-8.13 with 4.68×10^{-18} times an effective fluence.

An approximate expression for the annealing of the strain hardening exponent and other parameters which relate to the ductility of zircaloy was obtained by modifying the expression which has just been discussed. Tables of the strain hardening exponent after each transient anneal were constructed and compared with values predicted by substituting the effective cold work and fast neutron fluences into the MATPRO correlation for the effect of cold work and fast neutron fluence on the strain

[a] The 13.9 K/sec anneals to 811 and 866 K were used to find these values of Q and B .

hardening exponent^[B-8.1]. The best fit to the data was obtained by increasing the rate constant, B, fifty-fold in order to describe the annealing of the effective fast neutron fluence for the strain hardening exponent.

8.5.4 Comparison of Model With Data. Tables 8.IX through 8.XI are comparisons of the predicted strength coefficients and strain hardening coefficients with the data base used to construct the annealing models. The limited data for unirradiated cladding appear in Table 8.IX. Strength coefficients are predicted accurately but the strain hardening exponent is systematically underpredicted by the model.

Predicted strength coefficients for the transient anneals of irradiated cladding shown in Table 8.X are generally higher than the measured values when the maximum temperature is 894 K or higher. This trend may be interpreted to mean either that the temperature dependence of the annealing rate in the model^[a] is not sufficiently sensitive to temperature or that the irradiation damage is in fact made up of two or more components, one of which begins to anneal only at very high temperatures. The strength coefficient data for the isothermal anneals (Table 8.XI) do not confirm the trend toward overpredicting strengths at high temperature. Therefore the most successful interpretation of the trend would probably be the two component approach.

Predicted strain hardening exponents for annealed irradiated cladding are smaller than the measured values. This problem has not been addressed because it stems from the tendency of the model for the effect of irradiation and cold work to over predict the change of the strain hardening exponent due to cold work and irradiation at 644 K. A sensible effort to modify the model for the effect of irradiation and cold work would require analysis of true stress-true strain data from several samples after varying fluence at temperatures near 644 K. Such data are presently not available.

[a] The temperature dependence is given by the factor $\exp\left(\frac{-Q}{T^m}\right)$ in equation B-8.12.

TABLE 8.IX

COMPARISON OF MODEL PREDICTIONS
WITH DATA BASE FOR UNIRRADIATED CLADDING

Heating Rate (K/sec)	Maximum Temperature (K)	Strength Coefficient (MPa)		Strain Hardening Exponent	
		From Data	Predicted	From Data	Predicted
as irradiated	644	524	Assumed	0.040	0.024
5.6	811	524	524	0.040	0.024
5.6	866	520	520	0.040	0.021
5.6	894	503	513	0.047	0.018
5.6	978	444	440	0.218	0.118
27.8	811	515	524	0.035	0.024
27.8	866	514	523	0.033	0.023
27.8	894	513	522	0.035	0.022
27.8	978	516	501	0.045	0.018

TABLE 8.X

COMPARISON OF MODEL PREDICTIONS WITH DATA BASE
FOR TRANSIENT ANNEALS OF IRRADIATED CLADDING

Heating Rate (K/sec)	Maximum Temperature (K)	Strength Coefficient (MPa)		Strain Hardening Exponent	
		From Data	Predicted	From Data	Predicted
as irradiated	644	750.7	764.4	0.040	0.012
as irradiated	644	781.5	764.4	0.039	0.012
as irradiated	644	763.4	764.4	0.028	0.012
as irradiated	644	828.9	826.5	0.037	0.012
0.6	700	758.5	764.0	0.021	0.012
0.6	755	728.5	732.0	0.027	0.014
0.6	811	651.8	605.0	0.023	0.015
0.6	894	397.0	447.7	0.091	0.058
0.6	978	370.1	409.9	0.088	0.075
5.6	700	732.4	764.4	0.020	0.012
5.6	755	769.4	760.6	0.024	0.013
5.6	811	676.5	719.8	0.023	0.012
5.6	866	405.5	622.1	0.029	0.012
5.6	894	385.8	565.2	0.047	0.009
5.6	978	407.1	441.3	0.100	0.042
13.9	755	816.5	762.9	0.024	0.013
13.9	811	739.7	744.0	0.022	0.013
13.9	866	680.5	680.1	0.025	0.013
13.9	894	514.9	631.9	0.021	0.011
13.9	978	384.9	486.2	0.056	0.020
27.8	755	755.4	764.4	0.021	0.012
27.8	811	830.7	753.7	0.027	0.013
27.8	866	772.4	714.0	0.027	0.013
27.8	894	681.8	678.6	0.026	0.012
27.8	978	411.6	538.2	0.034	0.006
27.8	1033	403.6	475.7	0.046	0.025
27.8	1144	458.7	439.0	0.083	0.037
27.8	1255	481.1	428.3	0.100	0.043

TABLE 8.XI

COMPARISON OF MODEL PREDICTIONS WITH DATA BASE
FOR ISOTHERMAL ANNEALS OF IRRADIATED CLADDING

Heating Rate (K/sec)	Maximum Temperature (K)	Strength Coefficient (MPa)		Strain Hardening Exponent	
		From Data	Predicted	From Data	Predicted
644	as irradiated	750.7	764.4	0.040	0.012
644	as irradiated	781.5	764.4	0.039	0.012
644	as irradiated	763.4	764.4	0.028	0.012
644	as irradiated	828.9	826.5	0.037	0.012
700	60	724.8	778.6	0.033	0.014
755	10	683.5	601.4	0.028	0.017
755	60	648.2	583.2	0.030	0.016
811	1	649.7	514.1	0.029	0.013
811	10	425.2	424.5	0.031	0.045
811	30	460.8	454.7	0.050	0.077
866	1	387.9	429.0	0.044	0.043
866	5	417.2	411.3	0.077	0.069
866	30	451.6	453.1	0.096	0.090
894	1	411.3	420.2	0.076	0.051
894	30	483.2	453.0	0.130	0.094
978	1	406.0	Assumed	0.074	0.061
978	30	452.5	Assumed	0.112	0.099

8.5.5 Recommendations for Future Modeling and Experiments. This section contains several suggestions for further work which the author believes would lead to an improved model for cladding plastic deformation. They are intended to promote discussion among specialists interested in cladding material properties. One of the principal problems in constructing an annealing model is the lack of information about the effect of cold work and varying amounts of irradiation on cladding properties at reactor operating temperatures. The present model for annealing contains no information other than tests on unirradiated material from the NRC standard lot of tubing and tests on a different lot of material irradiated to fast neutron fluences of about 4.4×10^{25} neutrons/meter². The model should be revised to provide a realistic description of the strength and ductility of material with fluences between zero and 4.4×10^{25} as soon as data are available.

Data from annealing tests on unirradiated cladding which duplicate more of the annealing schedules of the irradiated cladding would be helpful in assessing the effect of irradiation if the unirradiated material were from the same lot of cladding as the irradiated material. Considerable unnecessary scatter is introduced into the data base when different lots of tubing are used in the separate tests.

One of the principal uncertainties in the annealing model is the functional form of the temperature dependent factors. Since isothermal anneals are the most easily interpreted data, isothermal anneals should be performed on unirradiated cold worked material as well as irradiated cold worked material.

A major uncertainty in the current model is the behavior of irradiated and cold worked cladding for strains beyond uniform elongation. These strains are not in the data base of the model developed in this report. A similar difficulty with the MATPRO data base for unirradiated cladding is currently under attack but the author is aware of no plan to provide data relevant to true stress-true strain modeling of irradiated cladding taken to large strains during annealing. Since extrapolation of the

empirical stress-strain law in MATPRO to strains is very likely to produce large errors for irradiated material, some true stress-true strain data in the high strain region are needed.

Finally, the limited recrystallization data reported by BCL for some tests will be useful in modeling both recovery and recrystallization kinetics during annealing. This data should be included in the excellent tables of the other data which have been provided by BCL. Any other measurements of recrystallization which are available should be included.

8.5.6 Listing of the Subcode CKMN and Examples of Output. Table B-8.XII presents a listing of the MATPRO subcode CKMN. The subcode will replace the first sections of all prior versions of MATPRO codes which deal with plastic deformation and will return values of the strength coefficient, strain hardening exponent and strain rate sensitivity exponent to each of the several MATPRO codes which use these parameters. The CKMN subcode also returns end-of-time step values of effective coldwork for the strength coefficient, effective coldwork for the strain hardening exponent, effective fast neutron fluence the strength coefficient, and effective fast neutron fluence for the strain hardening exponent.

Figures B-8.1 through B-8.8 are examples of the predicted behavior of the strength coefficient and strain hardening exponent of cladding subjected to typical temperature transients. Figure B-8.1 is a plot of the 644 K (700°F) strength coefficient as a function of the maximum temperature achieved during anneals at 1 K/sec, 25 K/sec and 100 K/sec. The initial cold work and fast neutron fluence are 0.7 area reduction and 5×10^{25} neutrons/meter². The strength coefficient anneals at about 850K when the heating rate is 1K/sec and at about 950K when the heating rate is 100 K/sec. Figure B-8.2 is a repeat of Figure B-8.1 with zero fast neutron fluence. The initial strength is smaller and the annealing occurs at slightly higher temperatures than that of Figure B-8.1.

TABLE B-8.XII

LISTING OF THE SUBCODE CKMN

SUBROUTINE CKMN(CFLUX,DELH,CTEMP,RTEMP,DELOXY,FNCK,FNCN,CWKF,CWNF,
=RSTRAN,AK,AN,AM)

CKMN CALCULATES PARAMETERS FOR THE CLADDING EQUATION OF STATE
AS A FUNCTION OF FAST NEUTRON FLUX, TIME STEP SIZE, TEMPERATURE
RATE OF CHANGE OF TEMPERATURE, AVERAGE OXYGEN CONCENTRATION,
FAST NEUTRON FLUENCE, AND COLD WORK

CFLUX = INPUT FAST NEUTRON FLUX (NEUTRONS/((METER**2)(SEC)))

DELH = INPUT TIME STEP SIZE (SEC)

CTEMP = INPUT CLADDING MESHPOINT TEMPERATURE (DEG K)

RTEMP = INPUT AVERAGE RATE OF CHANGE OF TEMPERATURE
(DEGREES K/SEC)

DELOXY = INPUT AVERAGE OXYGEN CONCENTRATION EXCLUDING
OXIDE LAYER = AVERAGE OXYGEN CONCENTRATION OF
AS RECEIVED CLADDING (KG OXYGEN/KG ZIRCALOY)

FNCK = INPUT EFFECTIVE FAST FLUENCE FOR STRENGTH COEFFICIENT
AT TIME STEP START (NEUTRONS/(METER**2))

FNCN = INPUT EFFECTIVE FAST FLUENCE FOR STRAIN HARDENING
EXPONENT AT TIME STEP START (NEUTRONS/(METER**2))

CWKF = INPUT EFFECTIVE COLD WORK FOR STRENGTH COEFFICIENT
AT TIME STEP START ((METER**2)/(METER**2))

CWNF = INPUT EFFECTIVE COLD WORK FOR STRAIN HARDENING
EXPONENT AT TIME STEP START ((METER**2)/METER**2))

RSTRAN = INPUT TRUE STRAIN RATE (SEC**-1)

FNCK = OUTPUT EFFECTIVE FAST FLUENCE FOR STRENGTH COEFFICIENT
AT TIME STEP FINISH (NEUTRONS/(METER**2))

FNCN = OUTPUT EFFECTIVE FAST FLUENCE FOR STRAIN HARDENING
EXPONENT AT TIME STEP FINISH (NEUTRONS/(METER**2))

CWKF = OUTPUT EFFECTIVE COLD WORK FOR STRENGTH COEFFICIENT
AT TIME STEP FINISH ((METER**2)/(METER**2))

CWNF = OUTPUT EFFECTIVE COLD WORK FOR STRAIN HARDENING
EXPONENT AT TIME STEP FINISH ((METER**2)/METER**2))

AK = OUTPUT STRENGTH COEFFICIENT (NEWTONS/(METER**2))

AN = OUTPUT STRAIN HARDENING EXPONENT (UNITLESS)

AM = OUTPUT STRAIN RATE SENSITIVITY EXPONENT (UNITLESS)

THE EQUATIONS USED IN THIS SUBROUTINE ARE BASED ON DATA FROM
(1) C.P. WOODS, PROPERTIES OF ZIRCALOY-4 TUBING, WAPD-TM-585
(1966)

(2) ULTIMATE STRENGTH DATA OF H.C. GRASSFIELD, ET AL. USAEC REPORT
GENP-482(1968)

(3) A.L. BEMENT, JR., EFFECTS OF COLD WORK AND NEUTRON
IRRADIATION ON THE TENSILE PROPERTIES OF ZIRCALOY-2,
USAEC REPORT HW-74955

(4) A. COWAN AND W.J. LANGFORD J. NUCLEAR MATER.

TABLE B-8.XII (continued)

30 271-2P1 (1969)

(5) L.M. HOWE AND W.R. THOMAS, J. NUCLEAR MATER.

1 (1961) 248

(6) A.M. GARDE IN ANL-75-58, LIGHT WATER REACTOR SAFETY
RESEARCH PROGRAM QUARTERLY PROGRESS REPORT APRIL - JUNE
1975 PAGES 47 - 83 (SEPTEMBER 1975)

(7) A.M. GARDE IN ANL-75-72, LIGHT WATER REACTOR SAFETY
RESEARCH PROGRAM QUARTERLY PROGRESS REPORT JULY-SEPTEMBER
1975

(8) R.L. MEHAN AND F.W. WIESINGER, MECHANICAL PROPERTIES
OF ZIRCALOY-2, KAPL-2110

(9) D. LEE AND W.A. BACKOFEN TMS-AIME 239 1034-1040 (1967)

(10) C.C. BUSBY AND K.J. MARSH, HIGH TEMPERATURE DEFORMATION
AND BURST CHARACTERISTICS OF RECRYSTALLIZED ZIRCALOY-4 TUBING,
WAPD-TM-900 (JANUARY 1976)

(11) A. A. BAUER, L. M. LOWRY, AND J. S. PERRIN, EVALUATING
STRENGTH AND DUCTILITY OF IRRADIATED ZIRCALOY. QUARTERLY
PROGRESS REPORT FOR APRIL THROUGH JUNE 1976,
BMI-NUREG-1956 (JULY 1976)

(12) A. A. BAUER, L. M. LOWRY, AND J. S. PERRIN, EVALUATING
STRENGTH AND DUCTILITY OF IRRADIATED ZIRCALOY. QUARTERLY
PROGRESS REPORT FOR JULY THROUGH SEPTEMBER, 1976, BMI-NUREG-1961
(OCTOBER 1976)

(13) A. A. BAUER, L. M. LOWRY, AND J. S. PERRIN, EVALUATING
STRENGTH AND DUCTILITY OF IRRADIATED ZIRCALOY. QUARTERLY
PROGRESS REPORT FOR OCTOBER THROUGH DECEMBER 1976,
BMI-NUREG-1967 (JANUARY 1977)

FNCK, FNCN, CWKF, AND CWNF ARE UPDATED BY EACH CALL.
PROGRAMS WHICH ITERATE USING SEVERAL CALLS SHOULD BE CERTAIN
TO INPUT CORRECT INITIAL VALUES OF THESE PARAMETERS

CODED BY D. L. HAGMAN AUGUST 1977

T = CTEMP

UPDATE FLUENCE

FNCK = FNCK + CFLUX * DELH

FNCN = FNCN + CFLUX * DELH

LIMIT STRAIN RATE TO A MINIMUM OF $1.0E-05$

IF(RSTRAN- $1.0E-5$) 3,4,4

3 RSTRAN = $1.0E-5$

FIND STRAIN RATE EXPONENT, AM, EXCEPT IN ALPHA - BETA REGION

4 IF(T-730.) 5,5,6

5 AM = $2.0E-2$

TABLE B-8.XII (continued)

```

GO TO 9
6 IF(T-900.) 7.8.8
7 A = 20.23172161
  B = - 0.07704552983
  C = 9.504843067E-06
  D = -3.860960716E-08
  AM = A + T*(B+ T*(C+ D*T))
GO TO 9
8 AM = -6.47E-2+T*2.203E-4
9 AM = AM * EXP(-69.*DELOXY)

C
C
C
ANNEALING MODEL
IF(T .LE. 5.0E+02) GO TO 12
IF(CWKF .LE. 1.0E-20) GO TO 10
OK = 2.33E+18
BK = (1.504E+00) * (1.0E+00 + (2.2E-25) * FNCK)
DISOK = OK * RTEMP * DELH * (T**(-7)) * 6.0
IF(ABS(DISOK) .LT. 1.0E-04) FNISOK = 1.0
IF(ABS(DISOK) .GE. 1.50E+02) GO TO 2
IF(ABS(DISOK) .GE. 1.0E-04) FNISOK = (EXP(DISOK) - 1.0)/DISOK
CWKF = EXP(-BK * DELH * EXP(-OK * (T**(-6)))) * FNISOK * CWKF
10 IF(CWNF .LE. 1.0E-20) GO TO 11
QN = 2.33E+18
BN = (1.504E+00) * (1.0E+00 + (2.2E-25) * FNCK) * 10.0
DISON = QN * RTEMP * DELH * (T**(-7)) * 6.0
IF(ABS(DISON) .LT. 1.0E-04) FNISON = 1.0
IF(ABS(DISON) .GE. 1.0E-04) FNISON = (EXP(DISON) - 1.0)/DISON
IF(ABS(DISON) .GE. 1.50E+02) GO TO 2
CWNF = EXP(-BN * DELH * EXP(-QN * (T**(-6)))) * FNISON * CWNF
11 IF(FNCK .LE. 1.0E+14) GO TO 1
BKI = 2.11E-06
QKI = 5.35E+23
DISOKI = QKI * RTEMP * DELH * (T**(-09)) * 08.0
IF(ABS(DISOKI) .LT. 1.0E-04) FNISKI = 1.0
IF(ABS(DISOKI) .GE. 1.50E+02) GO TO 2
IF(ABS(DISOKI) .GE. 1.0E-04) FNISKI = (EXP(DISOKI) - 1.0)/DISOKI
FNCK = FNCK/1.0E+20
FNCK = (BKI * DELH * (EXP(-QKI * (T**(-08)))) * FNISKI
= + (FNCK)**(-1))**(-1.0/1.0))
FNCK = FNCK * 1.0E+20
1 IF(FNCK .LE. 1.0E+14) GO TO 12
BNI = PKI * 50.
QNI = QKI
FNISNI = FNISKI
FNCK = FNCK/1.0E+20
FNCK = (BNI * DELH * (EXP(-QNI * (T**(-08)))) * FNISNI
= + (FNCK)**(-1))**(-1.0/1.0))
FNCK = FNCK * 1.0E+20

```

TABLE B-8.XII (continued)

```

      GO TO 12
      2 WRITE 991
991 FORMAT(51H  TIME STEP TOO LARGE FOR CLADDING ANNEALING MODEL )
C
C   FIND STRAIN HARDENING EXPONENT, AN
12 AN = (-1.86E-02 + T*(7.11E-04 - T*7.721E-07)) *
      = (8.47E-01 * EXP(-3.92E+01*CWNF) + 1.53E-01 +
      = CWNF * (-9.16E-02 + CWNF *2.29E-01)) *
      = EXP(-((FNCN)**0.33)/(3.73E+07 + 2.0E+08*CWNF))
      IF(T .GE. 850.) AN = 0.027908
C
C   FIND STRENGTH COEFFICIENT, AK
      E = -8.152540534E09
      F = 3.368940331E07
      G = -4.317334084E04
      H = 1.769348499E01
      IF(T-730.) 13,13,14
13 AK = (1.0884E09- 1.0571E06*T) * (1.0 + 5.46E-01*CWKF)
      GO TO 16
14 IF(T .GE. 900.) GO TO 15
      AK = (E + T*(F + T*(G + T*H))) * (1.0 + 5.46E-01*CWKF)
      GO TO 16
15 AK = EXP(8.755E08 +(8.663E03/T))
16 IF(T - 802.) 17,17,18
17 AK = AK + (1.794E11 - T*2.21E09)*DELOXY
      GO TO 19
18 AK = AK + 2.158E09*DELOXY
19 AKIRR = (4.68E-18) * FNCK
      AK = AK + AKIRR
C
C   MODIFY STRAIN RATE EXPONENT, AM, IN ALPHA - BETA REGION
      IF(RSTRAN-6.34E-3) 20,100,100
20 IF(T-1090.) 100,100,21
21 IF(T-1255.) 22,100,100
22 IF(T-1172.5) 23,23,24
23 AM = AM + (6.78E-2*ALOG(6.34E-3/RSTRAN)*((T-1090.)/82.5))*
      = EXP(-69. * DELOXY)
      GO TO 100
24 AM = AM + (6.78E-2*ALOG(6.34E-3/RSTRAN)*((1255.-T)/82.5))*
      = EXP(-69. * DELOXY)
100 CONTINUE
      RETURN
      END

```

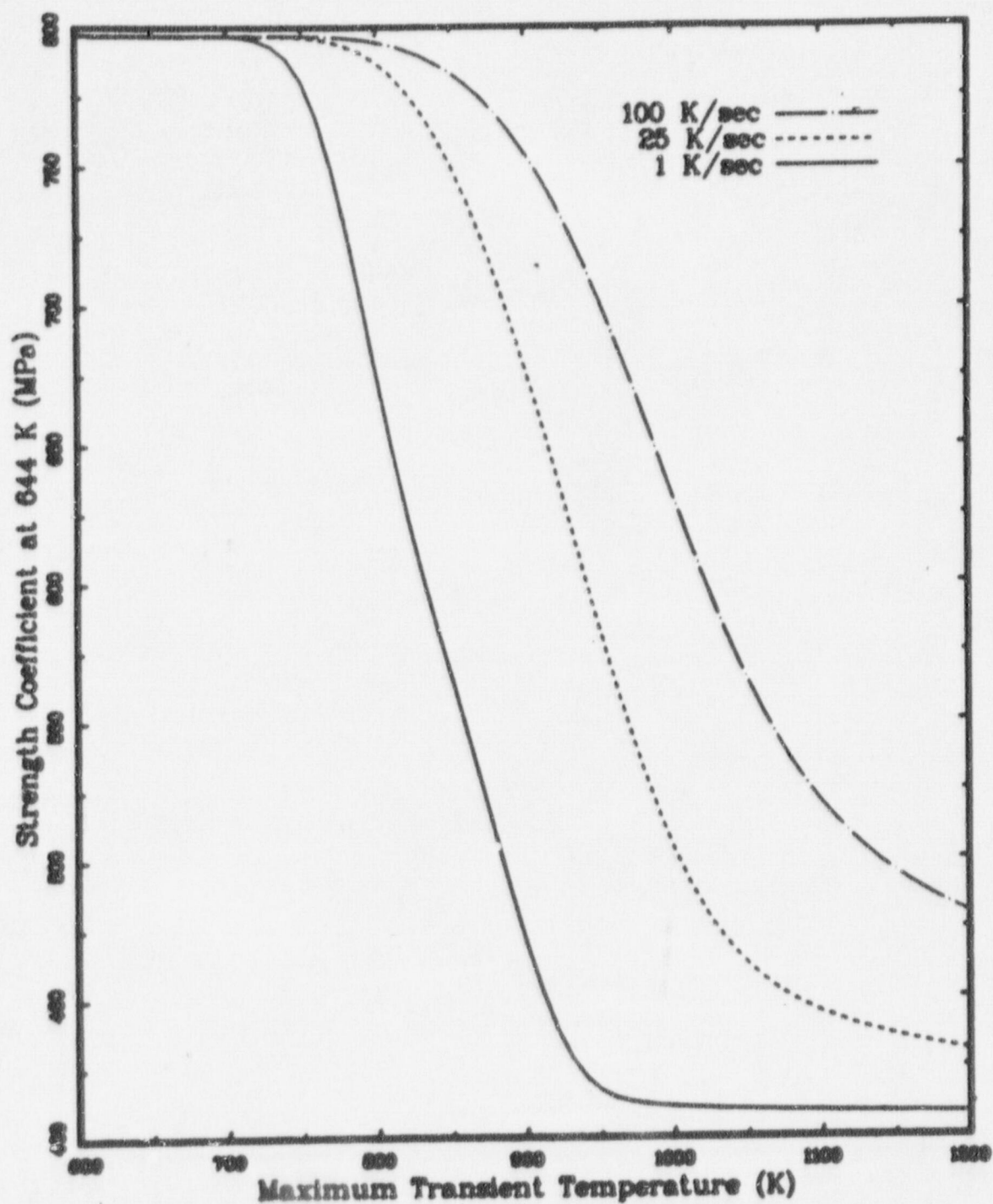


Fig. B-8.1 Predicted strength coefficient at 644 K of cladding with fast neutron fluence of 5×10^{25} neutrons/meter² and cold work of 0.7 as a function of the maximum temperature achieved during anneals at several heating rates.

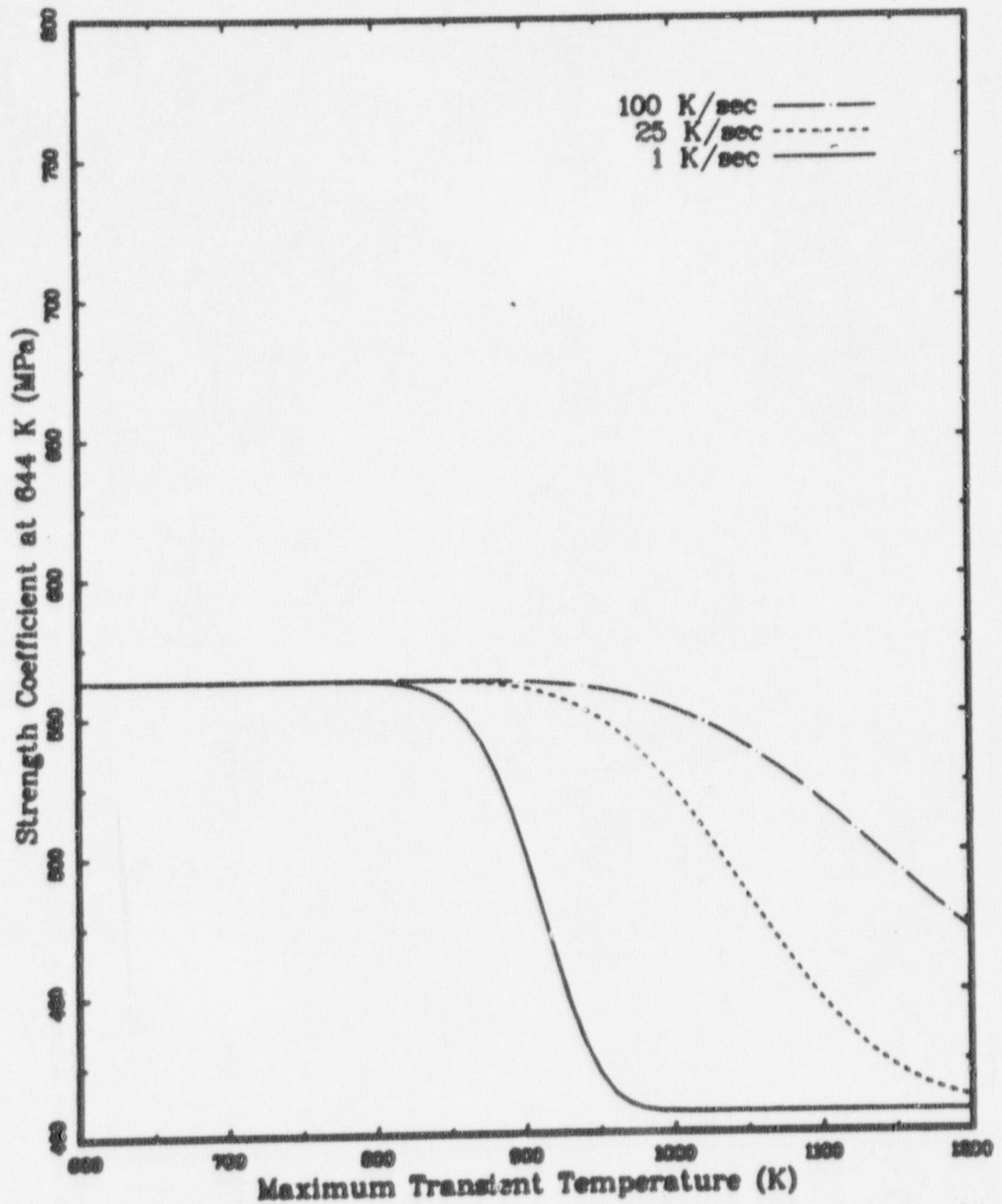


Fig. B-8.2 Predicted strength coefficient at 644 K of cladding with cold of 0.7 as a function of the maximum temperature achieved during anneals at several heating rates.

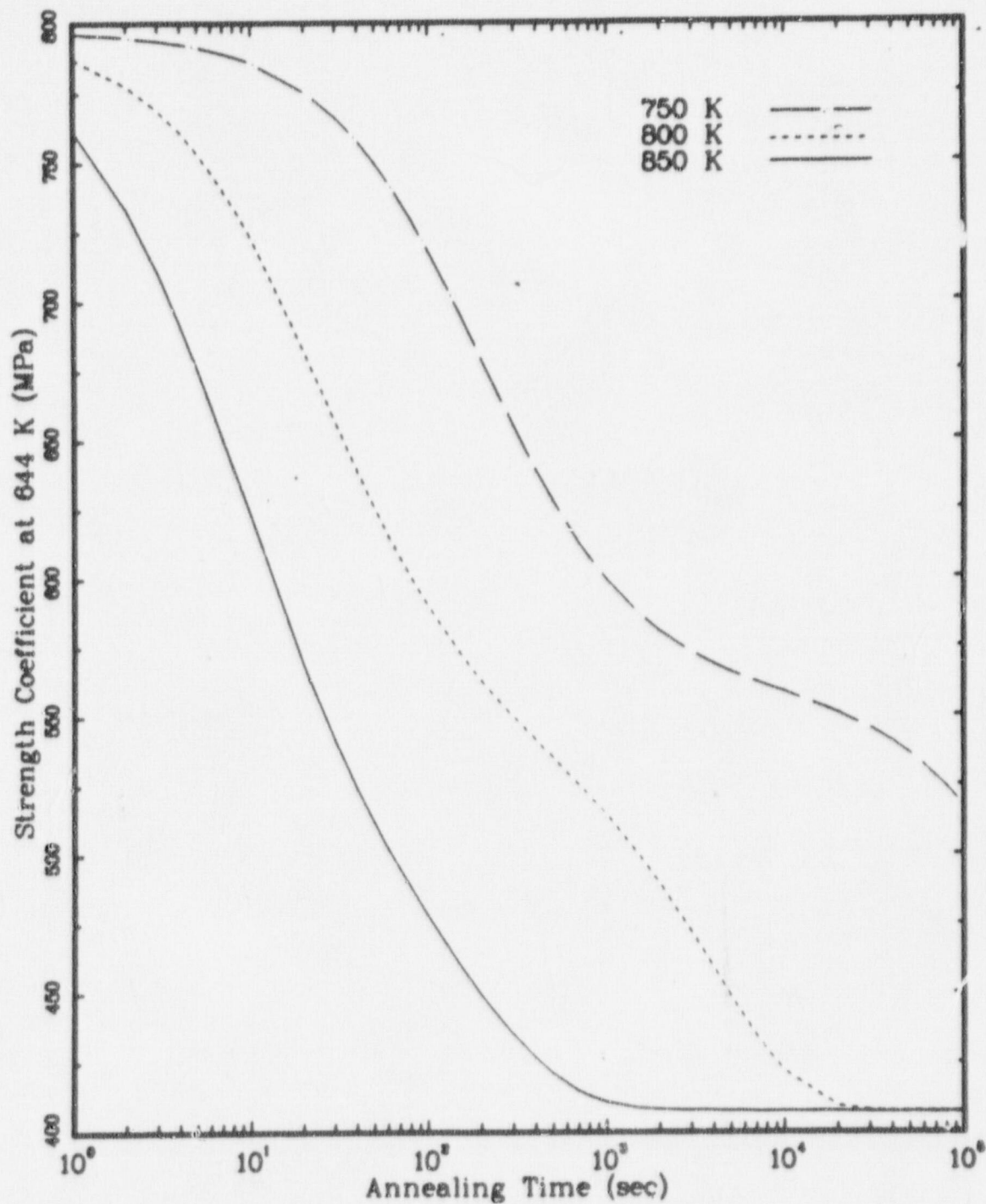


Fig. B-8.3 Predicted strength coefficient at 644 K of cladding with fast neutron fluence of 5×10^{25} neutrons/meter and cold work of 0.7 as a function of time for several isothermal anneals.

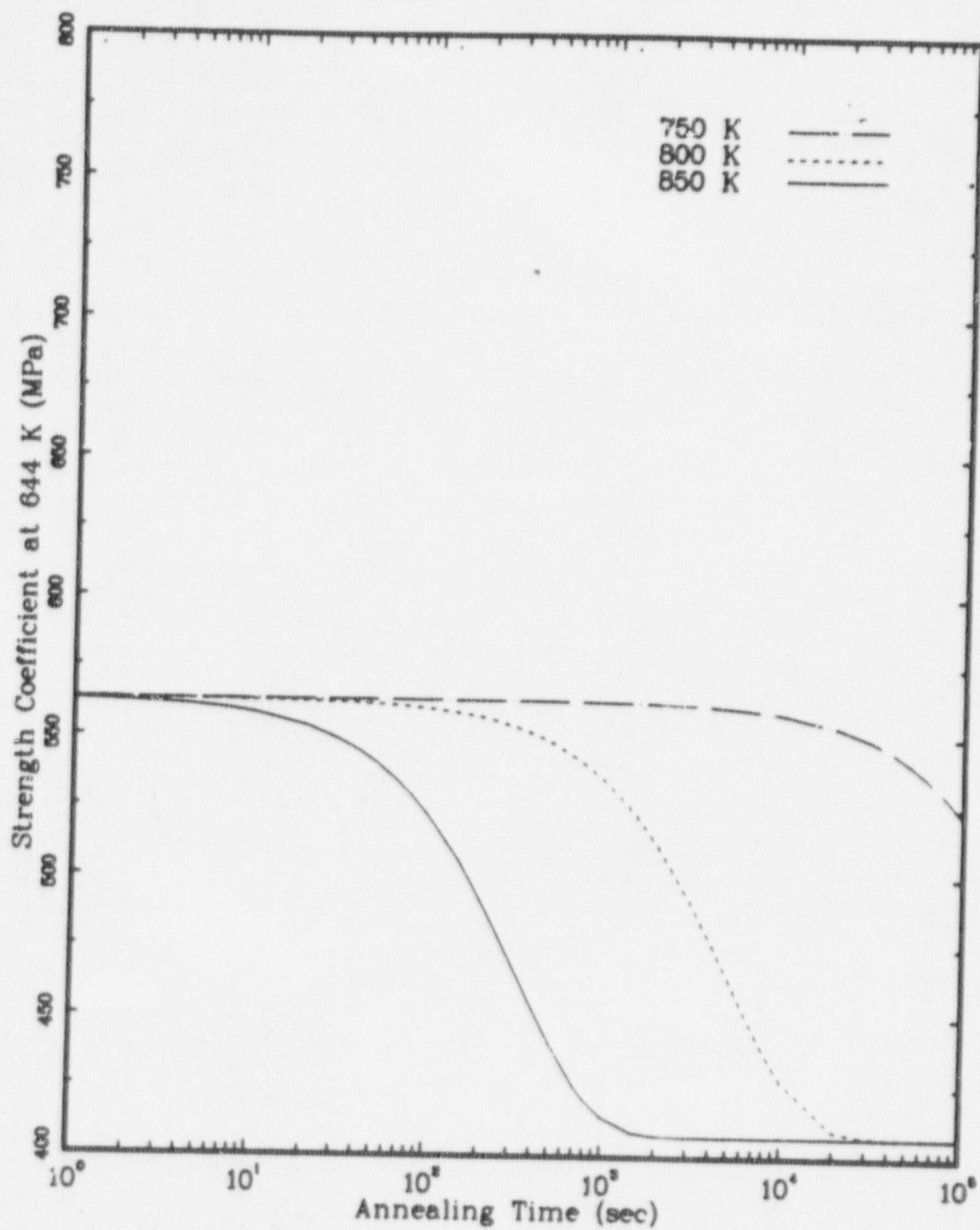


Fig. B-8.4 Predicted strength coefficient at 644 K of cladding with cold work of 0.7 as a function of time for several isothermal anneals.

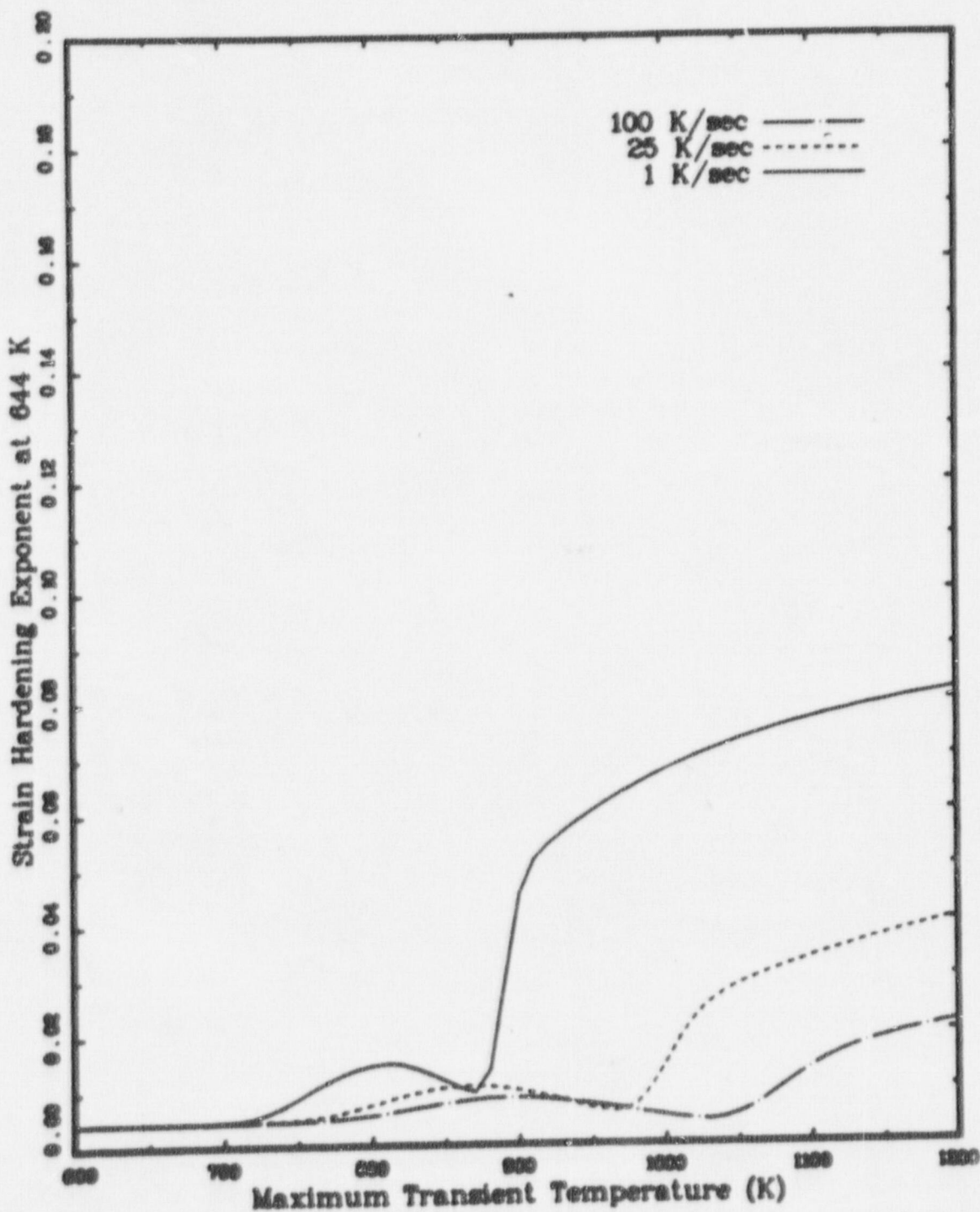


Fig. B-8.5 Predicted strain hardening exponent at 644 K of cladding with fast neutron fluence of 5×10^{25} neutrons/meter² and cold work of 0.7 as a function of the maximum temperature achieved during anneals at several heating rates.

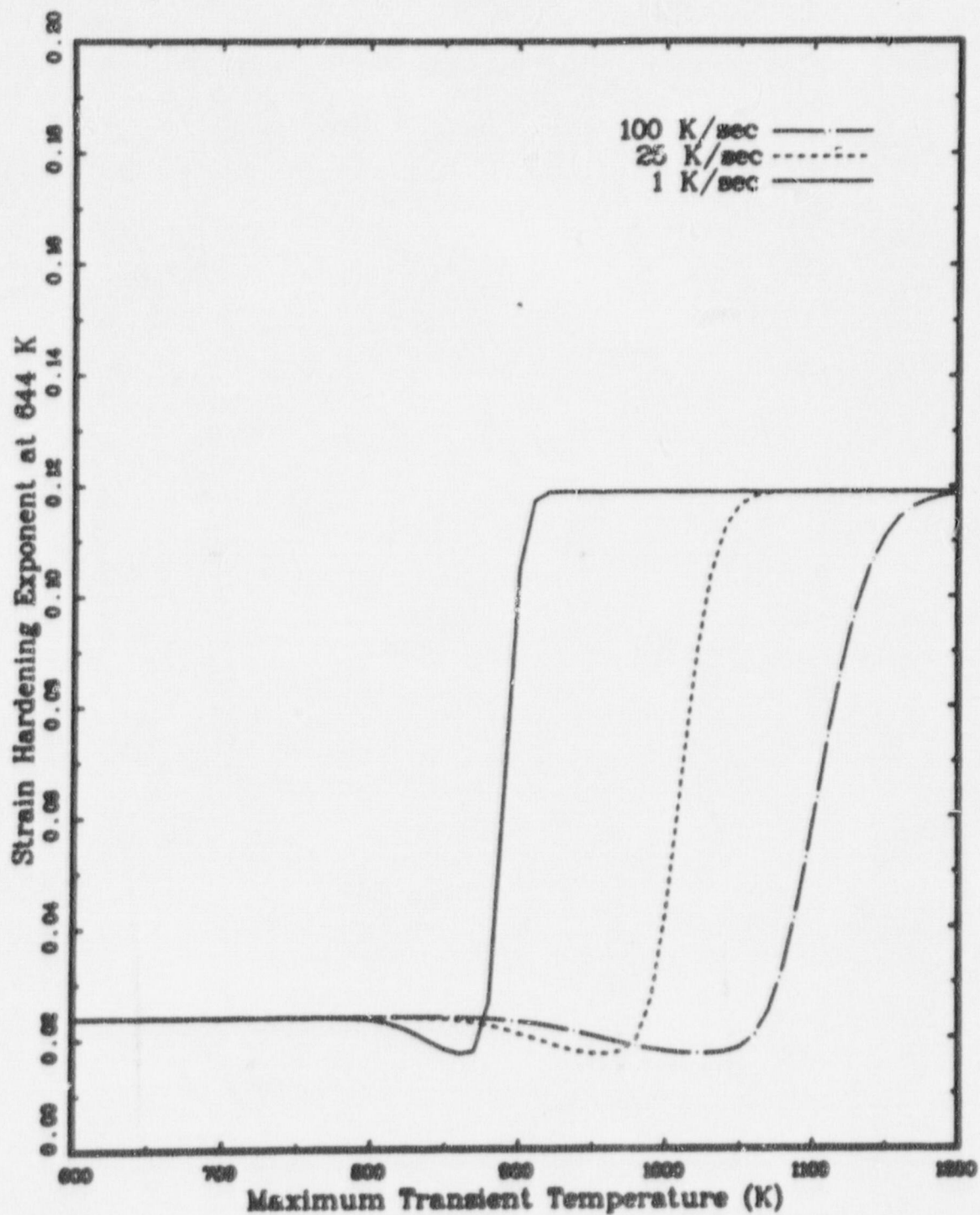


Fig. B-8.6 Predicted strain hardening exponent at 644 K of cladding with cold work of 0.7 as a function of the maximum temperature achieved during anneals at several heating rates.

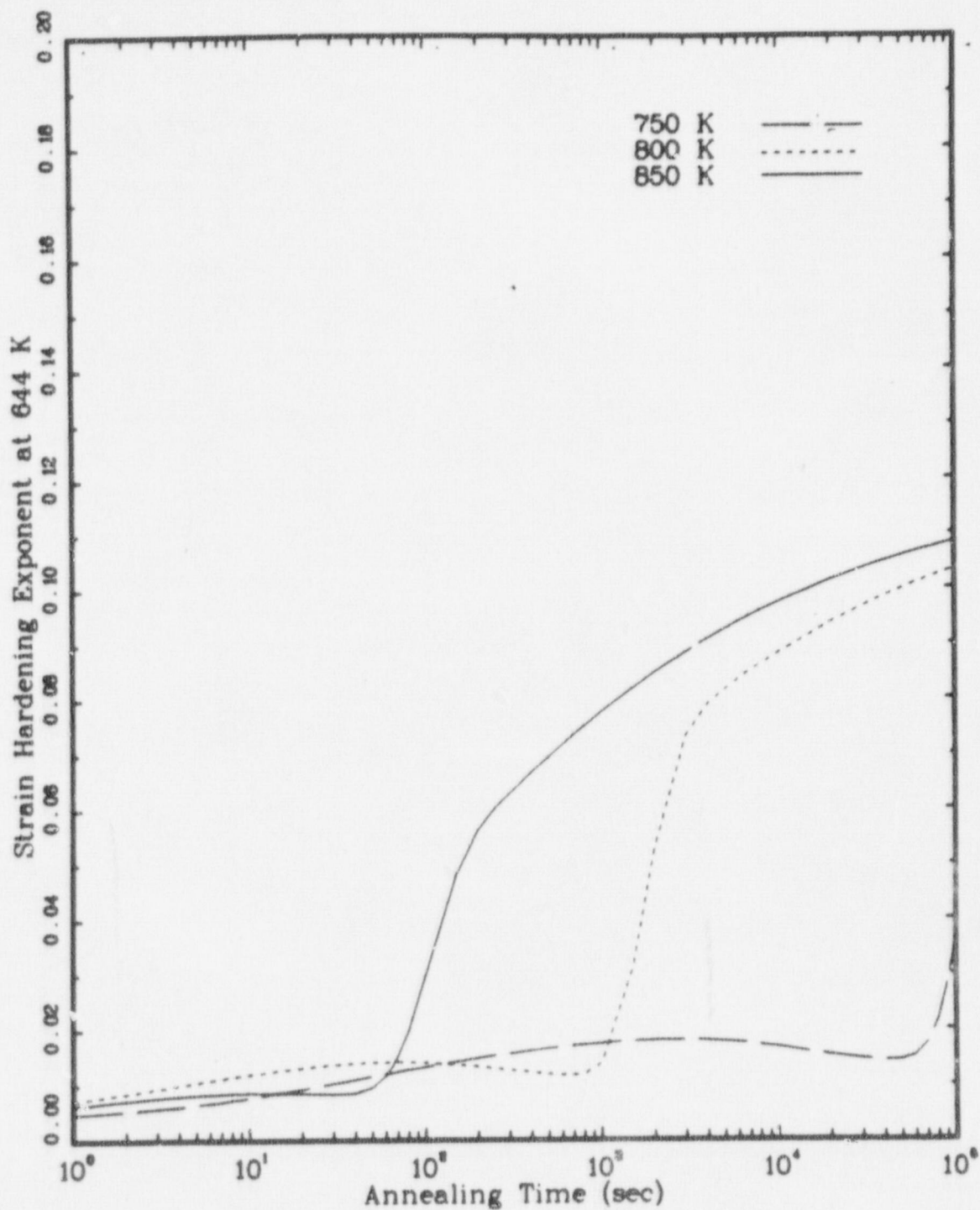


Fig. B-8.7 Predicted strain hardening exponent at 644 K of cladding with fast neutron fluence of 5×10^{25} neutrons/meter² and cold work of 0.7 as a function of time for several isothermal anneals.

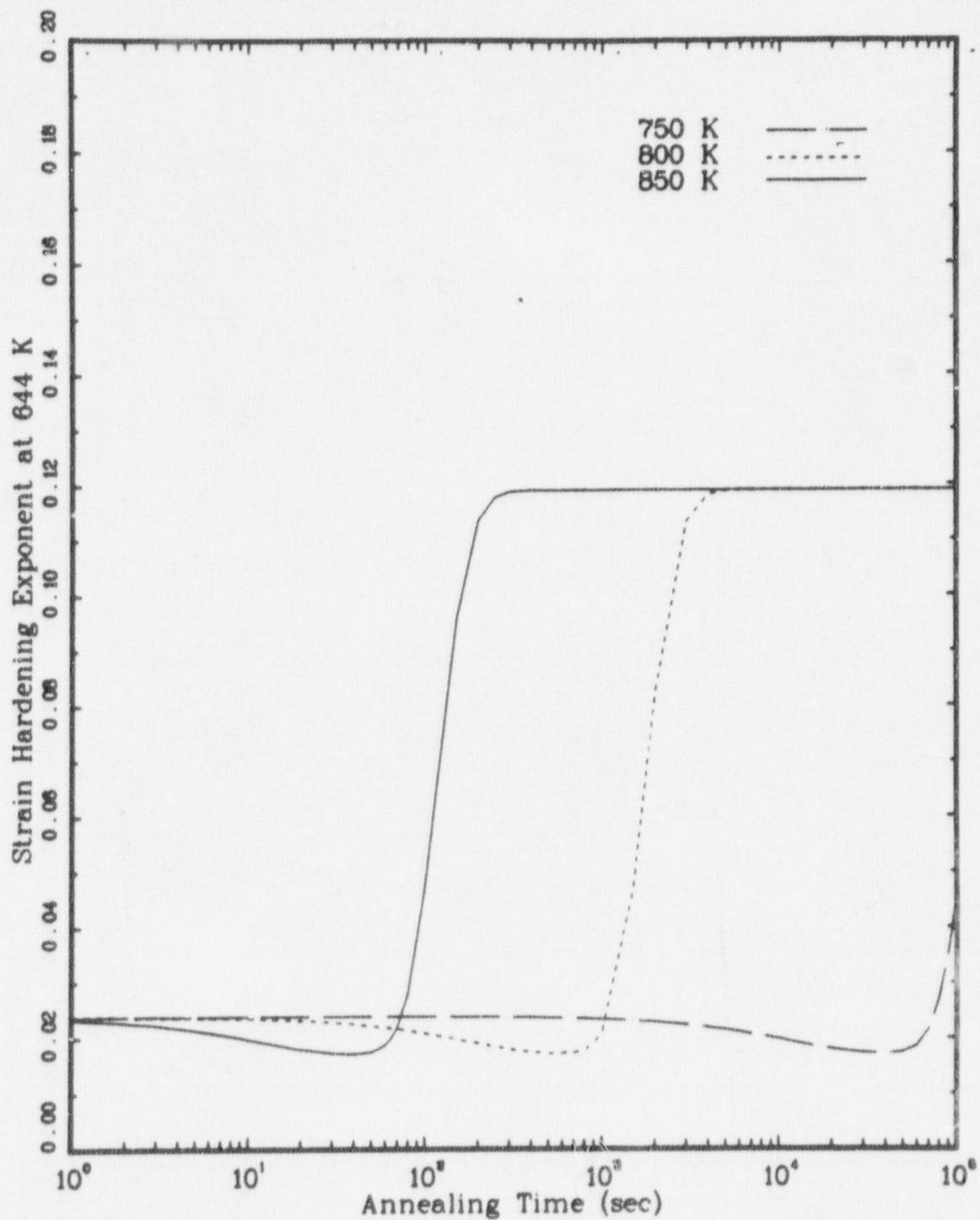


Fig. B-8.8 Predicted strain hardening exponent at 644 K of cladding with cold work of 0.7 as a function of time for several isothermal anneals.

Figures B-8.3 and B-8.4 show the effect of time at temperature on the strength coefficient for isothermal anneals at 850 K, 800 K and 750 K. Figure B-8.3 assumes an initial fast neutron fluence of 5×10^{25} neutrons/meter² and Figure B-8.4 assumes no initial fluence. The irradiated material anneals faster than the unirradiated material in spite of the fact that both begin with a cold work of 0.7 area reduction. The time axis has been extended to unrealistically long times to show completion of the 800 K anneal.

Figure B-8.5 shows the predicted transient annealing recovery of the strain hardening exponent of irradiated cladding for heating rates of 1, 25 and 100K/sec. Figure B-8.6 illustrates the recovery of the strain hardening exponent for unirradiated cladding. The strain hardening exponents decrease slightly then recover to their fully annealed values. The decrease corresponds to annealing of cold work.

Figures B-8.7 and B-8.8 illustrate the predicted recovery of the strain hardening exponent of irradiated and unirradiated cladding during isothermal anneals. The irradiated cold worked cladding of Figure B-8.7 recovers before the unirradiated cladding of Figure B-8.8.

8.6 REFERENCES

- B-8.1 D. L. Hagrman and G. A. Reymann, Cladding Stress Versus Strain, TFBP-TR-193 (April 1977).
- B-8.2 A. A. Bauer, L. M. Lowry, and J. S. Perrin, Progress on Evaluating Strength and Ductility of Irradiated Zircaloy During April Through June 1975, BMI-1935 (June 1975).
- B-8.3 A. A. Bauer, L. M. Lowry, and J. S. Perrin, Progress on Evaluating Strength and Ductility of Irradiated Zircaloy During July Through September, 1975, BMI-1938 (September 1975).
- B-8.4 A. A. Bauer, L. M. Lowry, and J. S. Perrin, Evaluating Strength and Ductility of Irradiated Zircaloy. Quarterly Progress Report for October Through December, 1975, BMI-1942 (December 1975).
- B-8.5 A. A. Bauer, L. M. Lowry, and J. S. Perrin, Evaluating Strength and Ductility of Irradiated Zircaloy. Quarterly Progress Report January Through March, 1976, BMI-1948 (March, 1976).
- B-8.6 A. A. Bauer, L. M. Lowry, and J. S. Perrin, Evaluating Strength and Ductility of Irradiated Zircaloy. Quarterly Progress Report April Through June, 1976, BMI-NUREG-1956 (July, 1976).
- B-8.7 A. A. Bauer, L. M. Lowry, and J. S. Perrin, Evaluating Strength and Ductility of Irradiated Zircaloy. Quarterly Progress Report July Through September, 1976, BMI-NUREG-1961 (October, 1976).
- B-8.8 A. A. Bauer, L. M. Lowry, and J. S. Perrin, Evaluating Strength and Ductility of Irradiated Zircaloy. Quarterly Progress Report October Through December, 1976, BMI-NUREG-1967 (January, 1977).

- B-8.9 A. A. Bauer, L. M. Lowry, and J. S. Perrin, Evaluating Strength and Ductility of Irradiated Zircaloy. Quarterly Progress Report January March, 1977, BMI-NUREG-1971 (April, 1977).
- B-8.10 L. M. Howe and W. R. Thomas, "The Effect of Neutron Irradiation on the Tensile Properties of Zircaloy-2", Journ. Nucl. Mat 2 (1960) pp 248-260.
- B-8.11 R. H. Chapman, Characterization of Zircaloy-4 Tubing Procured for Research Programs, ORNL/NUREG/TM-29 (July 1976).
- B-8.12 J. G. Byrne, Recovery, Recrystallization, and Grain Growth, New York: The Macmillan Company, 1965.

APPENDIX A

RELATION BETWEEN ISOTHERMAL AND TRANSIENT ANNEALING EXPRESSIONS

This appendix is a derivation of the expression used in the text to relate isothermal and transient annealing data. The rate equation discussed is the one which describes the annealing of the effect of cold work on the strength coefficient of cladding. However the method is the same for any of the several rate equations which are discussed in the main text of this report.

The equation assumed for the rate of change of the strength coefficient at some annealing temperature is

$$\frac{dK}{dt} = -B \left[\exp \left(\frac{-Q}{T^m} \right) \right] [K - K_A] \quad (B-A.1)$$

where K = strength coefficient of cold worked cladding^[a] (MPa)
 K_A = strength coefficient of annealed cladding^[a] (MPa)
 T = annealing temperature
 t = time
 B, Q, m = positive constants

[a] Measured at any standard test temperature.

If the annealing temperature is constant, equation B-A.1 can be integrated from an initial to a final time to obtain

$$\frac{K_{\text{final}} - K_A}{K_{\text{initial}} - K_A} = \exp \left(-B \left[t_{\text{final}} - t_{\text{initial}} \right] \exp \left(\frac{-Q}{T_m} \right) \right) \quad (\text{B-A.2})$$

In order to model annealing which occurs at non-constant temperatures, the time interval $t_{\text{final}} - t_{\text{initial}}$ is divided into η small intervals and the temperature during any small interval is assumed constant. The net change in K is the product of η terms like Equation B-A.2 for each interval

$$\frac{K_{\text{final}} - K_A}{K_{\text{initial}} - K_A} = \prod_{j=1}^{\eta} \exp \left(-B \left[\frac{t_{\text{final}} - t_{\text{initial}}}{\eta} \right] \exp \left(\frac{-Q}{T_j} \right) \right) \quad (\text{B-A3a})$$

$$\frac{K_{\text{final}} - K_A}{K_{\text{initial}} - K_A} = \exp \left(-B \left[\frac{t_{\text{final}} - t_{\text{initial}}}{\eta} \right] \prod_{j=1}^{\eta} \exp \left(\frac{-Q}{T_j} \right) \right) \quad (\text{B-A3b})$$

where T_j is the temperature during the j th interval

When the temperature change is a linear function of time, T_j in equation B-A3 can be obtained by interpolation between the initial and final temperatures.

The linear interpolation^[a], a Taylor series expansion, and a power series summation yield the result desired.

$$\prod_{j=1}^n \exp\left(\frac{-Q}{T_j^m}\right) = \prod_{j=1}^n \exp\left(\frac{-Q}{\left[T_f - 1/2\left(\frac{T_f - T_i}{\eta}\right) - (n-j)\left(\frac{T_f - T_i}{\eta}\right)\right]^m}\right) \quad (\text{B-A4a})$$

$$\prod_{j=1}^n \exp\left(\frac{-Q}{\left[T_f - 1/2\left(\frac{T_f - T_i}{\eta}\right)\right]^m} \left[1 + \frac{m(n-j)}{T_f - 1/2\left(\frac{T_f - T_i}{\eta}\right)} \frac{T_f - T_i}{\eta} + \dots\right]\right) \quad (\text{B-A4b})$$

$$= \exp\left(\frac{-Q}{\left[T_f - 1/2\left(\frac{T_f - T_i}{\eta}\right)\right]^m}\right) \prod_{j=1}^n \exp\left(\frac{m(n-j)}{\left[T_f - 1/2\left(\frac{T_f - T_i}{\eta}\right)\right]^{m+1}} \frac{T_f - T_i}{\eta}\right) \quad (\text{B-A4c})$$

[a] The interpolation may start with the final temperature as is done here:

$$T_j = T_i + 1/2 \left[\frac{T_f - T_i}{\eta} \right] - [n-j] \left[\frac{T_f - T_i}{\eta} \right]$$

or it may start with the initial temperature so that

$$T_j = T_i + 1/2 \left[\frac{T_f - T_i}{\eta} \right] + j \left[\frac{T_f - T_i}{\eta} \right]$$

The second form was used for coding the annealing model because it yields a result in terms of the initial temperature.

$$= \left[\exp \left(\left[T_f^{-1/2} \left(\frac{T_f - T_i}{\eta} \right) \right]^m \right) \right] \left[\frac{1 - \exp \left(\frac{-m(T_f - T_i) Q}{\left[T_f^{-1/2} \left(\frac{T_f - T_i}{\eta} \right) \right]^{m+1}} \right)}{1 - \exp \left(\frac{-m(T_f - T_i) Q}{\eta \left[T_f^{-1/2} \left(\frac{T_f - T_i}{\eta} \right) \right]^{m+1}} \right)} \right] \quad (\text{B-A4d})$$

If equation B-A4d is substituted into equation B-A3b and the limit as $\eta \rightarrow \infty$ is taken the resultant expression is

$$\frac{K_{\text{final}} - K_A}{K_{\text{initial}} - K_A} = \exp \left(-B \left[t_{\text{final}} - t_{\text{initial}} \right] \left[\exp \left(\frac{-Q}{T_j^m} \right) \right] \left[\frac{1 - \exp \left(\frac{-m(T_f - T_i) Q}{T_f^{m+1}} \right)}{\frac{m(T_f - T_i) Q}{T^{m+1}}} \right] \right) \quad (\text{B-A5})$$

Equation B-A5 is the same as equation B-8.9 of the main text. It differs from the isothermal form of the expression by the presence of the last factor in large square brackets.